Electrochemical Characterization of Two Perylenetetracarboxylic Diimides: Langmuir−Blodgett Films and Carbon Paste Electrodes

V. Parra,[†] T. Del Caño,[‡] M. L. Rodríguez-Méndez,[†] J. A. de Saja,[‡] and R. F. Aroca*,[‡]

Department of Inorganic Chemistry, E.T.S. Ingenieros Industriales, and Department of Condensed Matter Physics, Faculty of Sciences, University of Valladolid, s/n. 47011 Valladolid, Spain

Received August 21, 2003. Revised Manuscript Received November 11, 2003

The cyclic voltammograms (CV) of *N*,*N*′-bis(propyl)-3,4,9,10-perylenebis(dicarboximide) [PTCDIPr] and *N*,*N*′-bis(neopentyl)-3,4,9,10-perylenebis(dicarboximide)[BNPTCD] in Langmuir−Blodgett (LB) films, in carbon paste electrode (CPE), and in solution for BNPTCD are reported here for the first time. The data allow a comparison of the electrochemical behavior of highly organized LB films with the results obtained on CPE, where the active molecules are randomly dispersed in a carbonaceous matrix. The electrochemical reduction waves indicate the reversible formation of stable radical anions and dianions. The discussion of reduction potentials is integrated with spectroscopic data and the HOMO−LUMO energy positions of both materials obtained from density functional theory computations.

1. Introduction

Perylenetetracarboxylic diimide (PTCD) organic derivatives have been extensively studied due to their strong absorption and fluorescence, electroactive and photoactive properties, and good thermal, chemical, and photochemical stability.[1−8] Moreover, PTCD dyes and pigments usually exhibit a clear tendency to aggregate by stacking, a self-alignment that facilitates the fabrication of ordered thin films using vacuum evaporation or Langmuir−Blodgett (LB) techniques.[9] PTCDs primarily exhibit n-type conducting behavior as thin solid films,[2] and thereby, they have been successfully tested with dissimilar organic semiconductors such as phthalocyanines in thin film p−n heterojunction diodes.[10−12] The applications of PTCDs continue to be explored in thin film molecular electronics and as the main active components in sensors, photovoltaic cells, and electroluminescent devices.[10,13−15]

Perylenediimides, due to their large electron affinity, can go through electrochemical reduction at modest potentials, leading to the formation of stable radical anions, or even dianions.[5] This interesting property of perylenediimides could lead to applications as precursors for chemiluminescence, near-infrared emitters, and electrochromic materials.[13−15] There have been several studies of the electrochemical behavior of perylenediimides.[5,11,16−19] The majority of work has been carried out in solution, and the literature for solid state and thin solid films is scarce.[18,20−22]

The objective of the present work was to study the cyclic voltammetry of two distinct perylenetetracarboxylic diimide derivatives in solutions, as thin solid films prepared using the LB technique[9] and in the solid state with the PTCD material in a carbon paste electrode,

* Corresponding author. On leave from the University of Windsor, Windsor, Canada. E-mail: g57@uwindsor.ca.
[†] Department of Inorganic Chemistry.
[‡] Department of Condensed Matter Physics.

(1) Forrest, S. R. *Chem. Rev.* **1997**, *97*, 1973.
(2) Horowitz, G.; Kouki, F.; Spearman, P.; Fichou, D.; Nogues, C.; Pan, X.; Garnier, F. *Adv. Mater* **1996**, *8*, 242−244.
(3) Tasch, S.; List, E. J. W.; Hochfilzer, C.; Leising, G.; Rohr, U.; Schlichting, P.; Geerst, Y.; Scherft, A.; Müllen, K. *Phys. Rev. B* **1997**, *56*, 4479.
(4) Schlettwein, D.; Back, A.; Schilling, B.; Fritz, B.; Armstrong, N. R. *Chem. Mater.* **1998**, *10*, 601−612.
(5) Lee, K. L.; Zu, Y.; Herrmann, A.; Geerts, Y.; Müllen, K.; Bard, A. J. *J. Am. Chem. Soc.* **1999**, *121*, 3513−3520.
(6) Del Cano, T.; Duff, J.; Aroca, R. *Appl. Spectrosc.* **2002**, *56*, 744−750.
(7) Shklover, V.; Tautz, F. S.; Scholz, R.; Sloboshanin, S.; Sokolowski, M.; Schafefer, J. A.; Umbach, E. *Surf. Sci.* **2000**, *454−456*, 60−66.
(8) Aroca, R.; Del Cano, T.; de Saja, J. A. *Chem. Mater.* **2003**, *15*, 38−45.
(9) Petty, M. C. *Langmuir−Blodgett Films. An Introduction*; Cambridge University Press: Cambridge, 1996.
(10) Tang, C. W. *Appl. Phys. Lett.* **1986**, *48*, 183.
(11) Oekermann, T.; Schlettwein, D.; Wöhrle, D. *J. Appl. Electrochem.* **1997**, *27*, 1172−1178.
(12) Danziger, J.; Dodelet, J. P.; Lee, P.; Nebesny, K. W.; Armstrong, N. R. *Chem. Mater.* **1991**, *3*, 821.
(13) Williams, M. E.; Murray, R. W. *Chem. Mater.* **1998**, *10*, 3603−3610.
(14) Gosztola, D.; Niemczyk, M. P.; Svec, W.; Lukas, A. S.; Wasielewski, M. R. *J. Phys. Chem. A* **2000**, *104*, 6545−6551.
(15) Angadi, M. A.; Gosztola, D.; Wasielewski, M. R. *J. Appl. Phys.* **1998**, *83*, 6187−6189.
(16) Lu, W.; Gao, J. P.; Wang, Z. Y.; Qi, Y.; Sacripante, G. G.; Duff, J. D.; Sundararajan, P. R. *Macromolecules* **1999**, *32*, 8880−8885.
(17) Ford, W. E.; Hiratsuka, H.; Kamat, P. V. *J. Phys. Chem.* **1989**, *93*, 6692−6696.
(18) Cho, K. J.; Shim, H. K.; Kim, Y. I. *Synth. Met.* **2001**, *117*, 153−155.
(19) Gregg, B. A.; Cormier, R. A. *J. Phys. Chem. B* **1998**, *101*, 9952−9957.
(20) Danziger, J.; Dodelet, J. P.; Armstrong, N. R. *Chem. Mater.* **1991**, *3*, 812−820.
(21) Tamizhmani, G.; Dodelet, J. P.; Côté, R.; Gravel, D. *Chem. Mater.* **1991**, *3*, 1046−1053.
(22) Slattery, D. K.; Linkous, C. A.; Gruhn, N. E.; Baum, J. C. *Dyes Pigments* **2001**, *49*, 21−27.

10.1021/cm0347786 CCC: $27.50
Published on Web 12/19/2003

denoted as CPE.[23,24] It is of general interest to compare the electrochemical characteristics of the solid state form as CPE, where perylenediimide molecules are randomly packed, with those found in a highly organized thin film, where molecular order is induced through the LB technique. Since the conduction type of the materials under study is defined by their frontier orbital positions, the half-wave potentials obtained by cyclic voltammetry (CV), $E_{1/2} = (E_{red} + E_{ox})/2$, were used to estimate the electron affinities. The results were then correlated with the values obtained by quantum chemical calculations.

2. Experimental Section

2.1. Materials. *N*,*N*′-Bis(propyl)-3,4,9,10-perylenebis(dicarboximide) (denoted as PTCDIPr) and *N*,*N*′-Bis(neopentyl)-3,4,9,10-perylenebis(dicarboximide) (denoted as BNPTCD) were kindly provided by Dr. James Duff from the Xerox Research Center of Canada. The synthesis and spectroscopic characterization of both materials have been previously reported.[6,25] Dichloromethane (DCM), acetonitrile (MeCN), *N*,*N*′-dimethylformamide (DMF), trifluororacetic acid (TFA), KCl, $LiClO_4$, $KClO_4$, and tetra *n*-butylammonium perchlorate (TBAP) were purchased from Aldrich. Ferrocene (Fc) was purchased from Fluka. All these products were used without further purification.

2.2. Computations. Molecular orbital calculations were carried out with the Gaussian98 suite of programs.[26] Density functional theory (DFT) method, at the B3LYP/6-31G level of theory, was used.

2.3. LB Film Characterization. The electronic absorption spectra of all solutions and LB films were recorded with a double beam UV−visible Shimadzu 2101 spectrometer. Reflection−absorption infrared spectra (RAIRS) were recorded using a Nicolet Magna IR 760 spectrometer equipped with a DTGS detector. The sample chamber was purged with N_2 for 1 h prior to measurements. The RAIRS spectra were recorded at an incident angle of 80°. The gold films (50 nm mass thickness) used as substrates for RAIRS measurements were prepared by high-vacuum deposition (Balzers SCD004). Photoluminescence measurements were carried out in a Renishaw Research Raman microscope system (RM2000) equipped with a Leica microscope (DMLM series) using the 514.5 nm argon ion laser line as the excitation source.

2.4. Langmuir−Blodgett (LB) Electrode Preparation. Glass slides (2.5 × 1 cm^2) coated with ITO (150 Ω/sq) were used as substrates for the LB deposition. The substrates were cleaned with acetone and sonicated in water for 5 min. The metallic contact was fixed with silver paste and an epoxy resin. For LB film-based electrode fabrication, solutions of BNPTCD and PTCDIPr in DCM/TFA (95:5) mixed solvent were prepared with initial concentrations of 1.1×10^{-4} and 7.5×10^{-5} mol L^{-1}, respectively. Solutions were placed in an ultrasonic sonicator prior to spreading to prevent molecular aggregation.

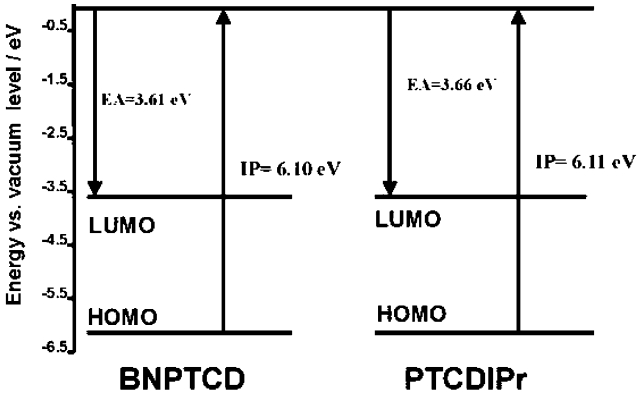

Figure 1. DFT-calculated energy level diagram for BNPTCD and PTCDIPr free molecules.

Films were fabricated using a KSV 5000 LB trough equipped with a Wilhelmy plate to measure the surface pressure. Monolayer characterization and isotherm stability tests, for both compounds, were carried out. The solutions were spread with a Hamilton microsyringe onto ultrapure distilled water (Millipore MilliQ, 18.2 Ω.cm resistivity), maintained at 20 °C. After evaporation of the solvent, the floating molecules were compressed at a speed of 8 mm min^{-1}. The monolayers were then transferred to the ITO electrode with a speed of 5 mm min^{-1} at a target surface pressure of 30 mN m^{-1} for PTCDIPr and 29 mN m^{-1} for BNPTCD, respectively. The target pressures were selected within the solid phase of the Langmuir monolayer. LB films of both compounds were fabricated using Z-deposition (i.e. transfer only during substrate upstroke). LB films of eight monolayers of BNPTCD and PTCDIPr were successfully made on the ITO substrates with transfer ratios near unity.

2.5. Carbon Paste Electrode (CPE) Preparation. The CPEs were prepared by mixing graphite powder (Ultracarbon, Ultra F purity) and the corresponding perylenediimide derivative (15% w/w). Nujol oil was used as a binder in the mixture. Paste was packed into the body of a 1 mL plastic syringe and compressed (surface area of 0.027 cm^2). A metallic wire was used as a contact. The CPEs were finally smoothed by hand over a clean filter paper prior to each experiment.

2.6. Electrochemical Measurements. Cyclic voltammetry (CV) was measured in an EG&G PARC Model 263A potentiostat/galvanostat (software M270) using a conventional three-electrode cell. The reference electrode was Ag/AgCl (KCl saturated) for water and Ag/Ag^+ (0.1 mol·L^{-1} $AgNO_3$ in MeCN) for organic solvents. A platinum disk (1 mm diameter) was used as the working electrode in solution experiments, and the perylenediimide-based CPEs or LB films on ITO-coated glass were used in the case of the solid-state voltammetry. The counter electrode was a platinum wire for solution and CPE measurements and a platinum plate (1.5 × 1 cm^2) when the working electrode was the LB film.

The solutions were prepared and introduced into a thermally isolated cell (Metrohm) with a temperature controlled liquid system (Neslab). All of them were deoxygenated by bubbling nitrogen through then for 10 min prior to use and maintained at constant temperature (20 °C).

3. Results andDiscussion

3.1. Computations. The DFT-calculated energy diagram for each molecule is shown in Figure 1. The ionization potentials (IPs), defined as the energy required to removing one electron from the highest occupied molecular orbital (HOMO), are found at 6.10 and 6.11 eV for BNPTCD and PTCDIPr, respectively. Ultraviolet photoelectron spectroscopy (UPS)[27] has been used to measure experimentally the IP of perylene-related compounds.[28,29] For 3,4,9,10-perylenetetracar-

(23) Kalcher, K.; Kauffman, J. M.; Wang, J.; Švancara, I.; Vytras, K.; Neuhold, C.; Yang, Z. *Electroanalysis* **1995**, *7*, 1.
(24) Nazri, M. Ph. D, University of Windsor, Windsor, Canada, 2003.
(25) Kam, A.; Aroca, R.; Duff, J.; Tripp, C. P. *Chem. Mater.* **1998**, *10*, 172−176.
(26) Frisch, M. J.; Trucks, G. W.; Schlegel, H. B.; Scuseria, G. E.; Robb, M. A.; Cheeseman, J. R.; Zakrzewski, V. G.; Montgomery, J. A., Jr.; Stratmann, R. E.; Burant, J. C.; Dapprich, S.; Millam, J. M.; Daniels, A. D.; Kudin, K. N.; Strain, M. C.; Farkas, O.; Tomasi, J.; Barone, V.; Cossi, M.; Cammi, R.; Mennucci, B.; Pomelli, C.; Adamo, C.; Clifford, S.; Ochterski, J.; Petersson, G. A.; Ayala, P. Y.; Cui, Q.; Morokuma, K.; Malick, D. K.; Rabuck, A. D.; Raghavachari, K.; Foresman, J. B.; Cioslowski, J.; Ortiz, J. V.; Stefanov, B. B.; Liu, G.; Liashenko, A.; Piskorz, P.; Komaromi, I.; Gomperts, R.; Martin, R. L.; Fox, D. J.; Keith, T.; Al-Laham, M. A.; Peng, C. Y.; Nanayakkara, A.; Gonzalez, C.; Challacombe, M.; Gill, P. M. W.; Johnson, B. G.; Chen, W.; Wong, M. W.; Andres, J. L.; Head-Gordon, M.; Replogle, E. S.; Pople, J. A. *Gaussian 98*; Gaussian, Inc.: Pittsburgh, PA, 1998.

Table 1. Experimental Electrochemical Data of BNPTCD in Different Solvents (vs Ag/$AgNO_3$ as Pseudoreference)

perylene	solvent	E_{red1}/E_{ox1} (V)	red 1 $E_{1/2}$ (V)	ΔE_{p1} (V)	E_{red2}/E_{ox2} (V)	red 2 $E_{1/2}$ (V)	ΔE_{p2} (V)
BNPTCD	DCM	−0.800/−0.730	−0.765	0.070	−0.950/−0.890	−0.920	0.060
	MeCN	−0.495/−0.255	−0.375	0.240	−0.605/−0.300	−0.452	0.305
	DMF	−0.410/0.075	−0.242	0.485	−0.560/−0.155	−0.357	0.405

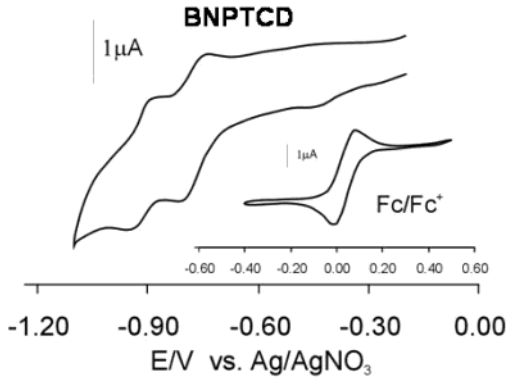

Figure 2. CV diagram of a ca. 10^{-5} mol·L^{-1} solution of BNPTCD in DCM, registered at 100 mV s^{-1}. The inset shows the CV response of a ferrocene solution in DCM (used as internal reference) registered at 100 mV s^{-1}.

boxylic dianhydride (PTCDA), UPS measurements established an IP of 6.46 eV,[28] and for 3,4,9,10-perylenetetracarboxylic bisimidazole (PTCBI) (a compound more closely related to the two PTCDs studied here), the value reported is 6.2 eV.[29] Therefore, the calculated IPs values at ca. 6.1 eV seems to be in good agreement with experiment. The electron affinity (EAs), the energy released when an electron is added to a molecule, for the free molecules, estimated from the LUMOs, is 3.61 eV for BNPTCD and 3.66 eV for PTCDIPr. The EA and, correspondingly, the LUMO energy level can be inferred experimentally from the first one-electron reduction process obtained in solutions and solid state (vide infra). The calculated HOMO and LUMO energy levels are similar for both compounds, indicating that the PTCD chromophore determines the electronic transitions and the lateral chains have a minor effect.[30] The energy gaps between the HOMO−LUMO orbital energies are 2.49 and 2.45 eV for BNPTCD and PTCDIPr, respectively, values in reasonable agreement with the visible absorption band observed in solutions *(*vide infra*)*.

3.2. Electrochemical Characterization. *3.2.1. CV in Solutions.* The voltammetry of BNPTCD was carried out using 10^{-5} mol L^{-1} solutions in DCM, MeCN, and DMF and adding 0.1 mol L^{-1} TBAP as supporting electrolyte. The poor solubility of PTCDIPr prevented solution voltammetry. CV diagrams for BNPTCD in DCM solutions exhibit two one-electron reduction steps, as can be seen in Figure 2. The reduction potential values are $E_{red1} = -0.80$ V and $E_{red2} = -0.95$ V and correspond to 1e-transfer processes, leading to the formation of a radical anion followed by that of the dianion.[5,31] These reduction potential peak values are in agreement with the earlier reported by Lee et al. for a series of perylenediimide derivatives.[5] The reduction data corroborate the strong electron-accepting nature of the carboxidiimide that brings the first reduction peak to a much lower negative value in comparison with that of perylene ($E_{red1} = -1.68$ V vs SCE),[32] in agreement with the fact that perylenediimide derivatives exhibit higher electron affinities than other perylene-based compounds.[2,16,33] Notably, the separation between first and second reduction peaks is considerably smaller (see Table 1) than the corresponding values reported for other aromatic compounds with diimides groups separated by a shorter ring spacer, such as naphthalene.[14] It must be concluded that the extended π-system in perylenediimides moderates the Coulomb repulsion between the electrons added during the first and the second reduction processes, allowing the formation of stable dianions.

To study the solvent effect on the voltammetric behavior, keeping TBAP as supporting electrolyte, the electron-donating[16] ability of the solvent was changed using DCM < MeCN < DMF. The results show that the CV responses of BNPTCD were shifted to positive potentials as the electron donor solvent character was increased (Table 1). Solvents with higher donor ability stabilize the imide anions to a greater extent, facilitating the imide reduction that will occur at more positive potentials.[16] In addition, the reverse oxidation processes were hindered when more donor solvent was used, supporting the assumption that the reduced species were stabilized.

The potentials were measured against Ag/$AgNO_3$ as the reference electrode, using the internal standard ferrocene/ferrocenium (Fc/Fc^+) redox system (inset in Figure 2). The experimental value for $E_{1/2} = (E_{red} + E_{ox})/2$ (the formal half-wave potential, avoiding kinetics effects, given in Table 1) obtained for Fc/Fc^+ vs Ag/$AgNO_3$ was 0.035 V at 100 mVs^{-1}. Using DCM as a solvent, and with the −4.5 eV and −4.8 eV values for NHE and Fc with respect to zero-vacuum level,[34−36] a value of 0.265 V for Ag/$AgNO_3$ vs NHE is obtained. Therefore, the LUMO energy value can be calculated using the following expression

$$E_{LUMO} = -4.5 \text{ eV} - e(E_{Ag/AgNO_3 \text{ vs NHE}} + E_{1/2}) \quad (1)$$

where $E_{1/2}$ is the half-wave potential of the first perylenediimide reduction.

(27) Ishii, H.; Sugiyama, K.; Ito, E.; Seki, K. *Adv. Mater* **1999**, *11*, 605.
(28) a)Schlaf, R.; Parkinson, B. A.; Lee, P. A.; Nebesny, K. W.; Armstrong, N. R. *J. Phys. Chem. B* **1999**, *103*, 2985. (b) Schlaf, R.; Schroeder, P. G.; Nelson, M. W.; Parkinson, B. A.; Lee, P. A.; Nebesny, K. W.; Armstrong, N. R. *J. Appl. Phys.* **1999**, *86*, 1499.
(29) Hill, I. G.; Schwartz, J.; Kahn, A. *Org. Electron.* **2000**, *1*, 5−13.
(30) Kavassalis, T. A.; Kazmaier, P. M.; Bareman, J. P.; Sundararajan, P. R.; Wright, J. D. *Ind. Eng. Chem. Res.* **1995**, *34*, 4174−4182.
(31) Mazur, S.; Lugg, P. S.; Yarnilzky, C. *J. Electrochem. Soc.* **1987**, *134*, 346.
(32) Parker, V. D. *J. Am. Chem. Soc.* **1976**, *98*, 98−103.
(33) Pösch, P.; Thelakkat, M.; Schmidt, H. W. *Synth. Met.* **1999**, *102*, 1110−1112.
(34) Nozik, A. J.; Memming, R. *J. Phys. Chem.* **1996**, *100*, 13061−13078.
(35) Reiss, H.; Heller, A. *J. Phys. Chem.* **1985**, *89*, 7−4213.
(36) Bard, A. J.; Faulkner, L. R. In *Electrochemical Methods. Fundamental and Applications*; Wiley: New York, 1980; pp Ch. 14, 634.

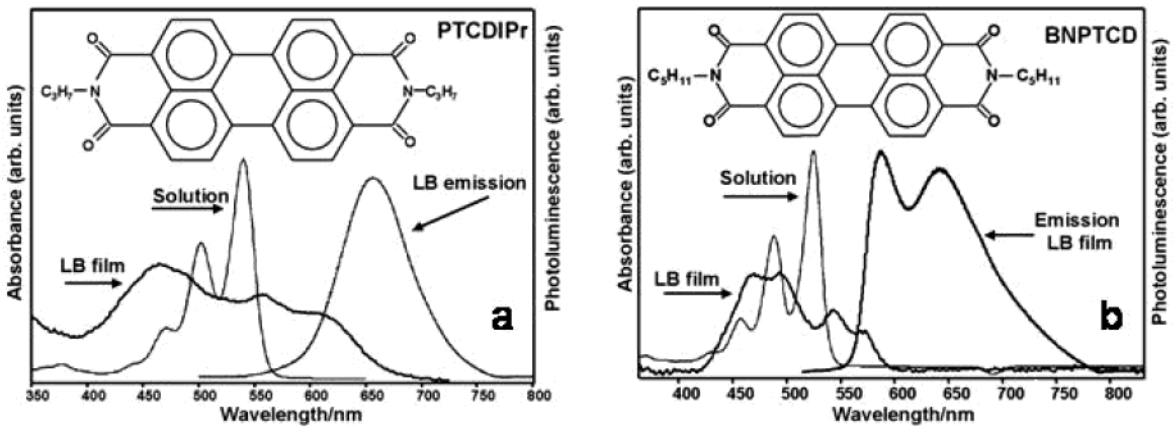

Figure 3. (a) Electronic absorption and emission spectra of PTCDIPr LB films and (b) BNPTCD LB film. Electronic absorption spectra of dilute solutions are also shown for both dyes.

The estimated LUMO energy value for BNPTCD in DCM solvent is, then, $E_{LUMO} = -4.5$ eV $-$ e[0.265 + (−0.765)] = −4.00 eV, referred to the zero-vacuum level. This estimation might vary in other solvents due to changes in donor ability, solvent dielectric constant, and solvation energy. From the estimated E_{LUMO} in DCM, a difference of ca. 0.4 eV with the DFT free molecule calculations ($E_{LUMO} = -3.61$ eV) is inferred. These differences could be explained by the nature of the theoretical calculations. The calculations are for systems in a vacuum and as free molecules; an environment that differs substantially from the experimental conditions, where solvent effects, ions, and molecular interactions play a decisive role in determining the properties. The calculations could have been carried out for molecular ions, i.e., the energy of a singly occupied LUMO following molecular structural relaxation. However, that computational task was beyond the scope of the present work. It is also possible that the differences could be attributed to the fact that electrochemical measurements usually underestimate the HOMO−LUMO gap and, thereby, overestimate EA when compared with single free molecule values.[12]

3.2.2. Langmuir−Blodgett (LB) Films. 3.2.2.1. LB Film Morphological and Spectroscopic Characterization. A complete morphological and spectroscopic characterization of Langmuir−Blodgett films of BNPTCD and PTCDIPr have been reported.[37] Reproducible surface pressure−area isotherms of the BNPTCD and PTCDIPr Langmuir films were obtained with well-defined solid phases. The areas per molecule, extrapolated to $\pi = 0$ for the Langmuir films, were 70 and 61 Å^2 for BNPTCD and PTCDIPr, respectively. Taking into account the size of the perylene and perylenediimides (ca. 8 Å width × 14 Å length), these area-per-molecule values require that the molecules for both derivatives organize with a tilted head-on arrangement on the water subphase. The overall head-on molecular organization found in Langmuir films is preserved when the BNPTCD and PTCDIPr monolayers are transferred onto substrates, as extracted from the reflection−absorption infrared spectra (RAIRS).[37] The electronic absorption and emission spectra of LB films of BNPTCD and PTCDIPr are shown in Figure 3a,b. The reference is the dilute solution absorption spectra showing the characteristic vibronic structure of the absorption band assigned to the $\pi-\pi^*$ electronic transitions of PTCDs.[38] The main 0−0 transition appears at 524 and 539 nm in BNPTCD and PTCDIPr, respectively. The 0−1, 0−2 vibronic progressions are found at 488 and 456 nm for BNPTCD and 501 and 468 nm for PTCDIPr. The fact that electronic absorption bands of the PTCDIPr are slightly shifted to higher wavelength values (ca. 15 nm for the 0−0 vibration band) is in agreement with the calculated values for the free molecules (see Figure 1). In the solid thin films, band broadening can be clearly observed as a result of molecular packing. The PTCDIPr LB film $\pi-\pi^*$ electronic absorption band presents three main components centered at 456, 556, and 612 nm. The absorption spectrum of the BNPTCD LB film exhibits a splitting of the $\pi-\pi^*$ electronic transition band with main peaks at 466, 499, and 543 nm and a marked shoulder at 569 nm. Direct comparison between solid thin film spectra shows that the absorption band of the PTCDIPr film appears considerably more red-shifted with respect to the solution (73 nm) than that of the BNPTCD film (45 nm). The emission spectra of BNPTCD and PTCDIPr LB films also show the difference in molecular stacking between derivatives. The spectrum of the PTCDIPr LB film consists of a broad featureless band with maximum centered at 657 nm (Figure 3a), which can be assigned to excimers as typically observed in bulk perylene materials, thin solid films,[39] and ultrathin films.[4] The BNPTCD LB film spectrum (shown in Figure 3b) exhibits two overlapping bands with maxima at 590 and 642 nm that correspond to monomer and excimer emission, respectively. Thus, the spectroscopic data suggest a weaker interaction between adjacent BNPTCD molecules, probably due to the hindering effect of the neopentyl groups that reduce stacking. The latter has been also confirmed using AFM (not shown),[37] where the topographical images of BNPTCD LB films showed higher porosity and less packing than those of PTCDIPr.

3.2.2.2. LB Films Electrochemical Characterization. LB Electrodes. The CV diagrams for LB films of perylene-

(37) Del Cano, T.; Parra, V.; Rodriguez-Méndez, M. L.; Aroca, R.; De Saja, J. A. *Org. Electron.* (in press). Work presented at the European Materials Research Society (E-MRS) Spring Meeting 2003.

(38) Adachi, M.; Murata, Y.; Nakamura, S. *J. Phys. Chem.* **1995**, *99*, 14240−14246.

(39) Yip, W. T.; Levy, D. H. *J. Phys. Chem.* **1996**, *100*, 11539−11545.

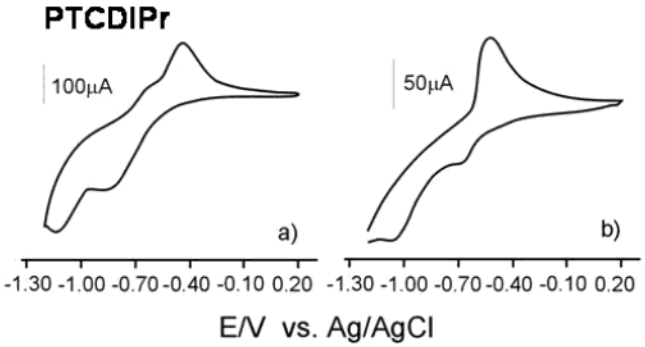

Figure 4. CV responses of PTCDIPr LB films (eight monolayers) immersed in (a) 0.1 mol·L^{-1} $LiClO_4$ and (b) 0.1 mol·L^{-1} KCl aqueous solutions. Scan rate = 100 mV·s^{-1}.

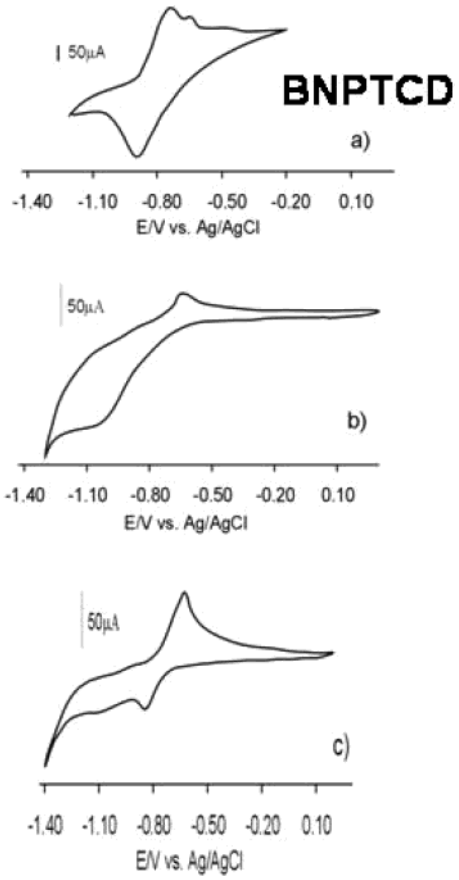

Figure 5. CV responses of BNPTCD LB films (eight monolayers) immersed in (a) 0.1 mol·L^{-1} $LiClO_4$, (b) 0.1 mol·L^{-1} $KClO_4$, and (c) 0.1 mol·L^{-1} KCl aqueous solutions. Scan rate = 100 mV·s^{-1}.

diimides (eight monolayers) coated on ITO electrodes in different aqueous solutions of $LiClO_4$, $KClO_4$, and KCl are shown in Figures 4 and 5. The results for LB films on ITO in organic solvents DCM, THF, DMF, and acetonitrile are not included. The LBs are partially soluble in these solvents, and consequently, CV responses diminished sharply after a few scans.

The CV diagrams of PTCDIPr LB films immersed in 0.1 mol L^{-1} solutions of KCl and $LiClO_4$ are shown in Figure 4a,b. The variations of the CV with the electrolyte is evident; however, in both supporting electrolytes, two reduction processes can be distinguished. The first reduction in $LiClO_4$ is quite different from that in KCl ($E_{red1} = -0.68$ V vs -0.83 V); however, the subsequent process was less affected by the electrolyte ($E_{red2} = -1.06$ and -1.13 V). Using KCl as supporting electrolyte, only one oxidation peak was recorded at $E_{ox} = -0.51$ V, a potential value located between the two values observed in $LiClO_4$ at $E_{ox2} = -0.64$ V and $E_{ox1} = -0.43$ V. The latter result suggests that the envelope of the oxidation peak in KCl corresponds to a two-electron-transfer process. Voltammograms on $LiClO_4$ showed corresponding non-Nernstian redox couples, indicating a slow rate for the charge-transfer reaction.

The effect of the size of electrolytic cations and anions on the reduction features of BNPTCD LB film seems to be even more remarkable than for PTCDIPr, as can be seen in Figure 5 for the voltammograms of LB on 0.1 mol L^{-1} aqueous $LiClO_4$, $KClO_4$, and KCl. In perchlorate solutions (Figure 5a,b), the reduction peak appears at a much more positive potential (-0.88 V) than in $KClO_4$ (-1.06 V). The relative peak intensity of the reverse anodic wave is more symmetrical for the Li^+ electrolyte than it is for the K^+ electrolyte. Furthermore, the separation between anodic and cathodic peaks is clearly larger in the presence of K^+ ions. These differences can be explained by taking into account the ionic radii of the counterions under study. The smaller size of Li^+ facilitates the BNPTCD reduction and makes the process more reversible. Further, the influence of the anion in the supporting electrolyte can also be seen by comparing the CV registered in KCl with that in $KClO_4$. It can be seen in Figure 5 that in the supporting electrolyte with chloride anion the one-electron reduction processes from the neutral BNPTCD species to the dianion state are clearly separated ($E_{red1} = -0.84$ V; $E_{red2} = -1.10$ V). The oxidation potentials for the different electrolytes are $E_{ox1} = -0.73$ V, -0.64 V, and -0.63 V for $LiClO_4$, $KClO_4$, and KCl, respectively. The results indicate that selection of the supporting electrolyte is an important factor in the electroanalysis of the LB films. The differences observed in the CV diagrams of the BNPTCD LB films immersed in different electrolytes must be attributed to the fact that the response clearly depends on the capability of the LB film to allow the flow of counterions at the electrode surface. In conclusion, the different electrochemical behavior of LB films of both perylenediimide derivatives is likely to be explained in terms of their diverse packing properties in LB films, and there is only a minor influence of the electronic nature of the *N*-substituents. Although BNPTCD and PTCDIPr molecules show similar preferential head-on orientation on LB films, the later exhibit a higher molecular stacking ability, since the attached neopentyl groups in BNPTCD partially prevent molecular packing. Thus, the lower molecular coupling of the BNPTCD films favors the flow of ions and, hence, the observed effect of the electrolyte on the CV results. The higher degree of molecular packing of PTCDIPr LB films compared to that of BNPTCD is also confirmed by the red-shifting found in the electronic absorption spectra (Figure 3): the $\pi-\pi^*$ electronic absorption band of PTCDIPr in the LB film is shifted ca. 70 nm to longer wavelengths with respect to the solution; meanwhile, in the case of BNPTCD, the red-shifting is just 45 nm.

A rough first estimation of the EA for BNPTCD and PTCDIPr in organized LB thin solid films can be obtained using the $E_{1/2}$ values and eq 1, taking as

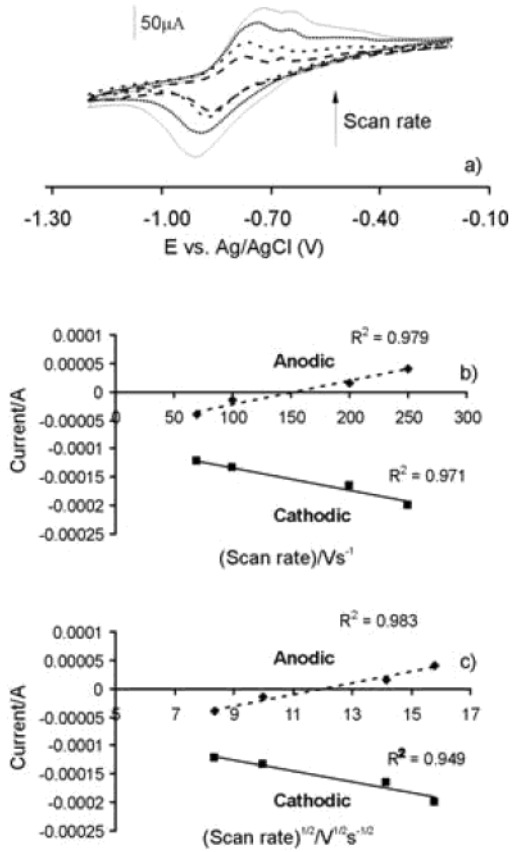

Figure 6. Effect of the scan rate in the CV responses (a) of a BNPTCD LB film (eight monolayers) immersed in 0.1 mol·L^{-1} $LiClO_4$ aqueous solution. The scan rate varies from 0.07 to 0.25 V·s^{-1}. Plots of scan rate effect on the anodic and cathodic peak currents. (b) Dependence on v and (c) dependence on $v^{1/2}$.

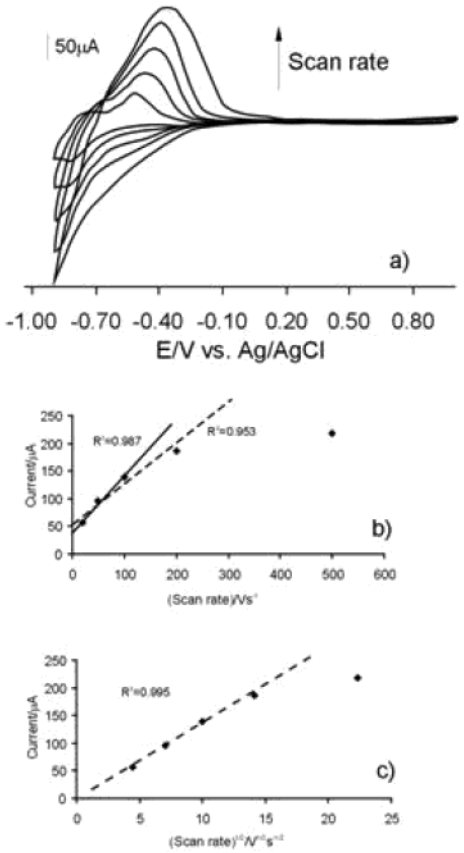

Figure 7. Effect of the scan rate on the CV response (a) of PTCDIPr-based CPE immersed in 0.1 mol·L^{-1} $LiClO_4$ aqueous solution. The scan rate varies from 0.07 to 0.50 V·s^{-1}. Plots of the scan rate effect on the anodic and cathodic peak currents. (b) Dependence on v and (c) dependence on $v^{1/2}$.

reference potential the Ag/AgCl vs NHE value of 0.222 V. Considering that $E_{1/2} = -(0.68 + 0.51)/2 = -0.59$ V in KCl and $E_{1/2} = -(0.83 + 0.43)/2 = -0.63$ V in $LiClO_4$ for PTCDIPr LB film, the calculated EA values fluctuate in the −4.09/−4.13 eV range. Similarly, for BNPTCD films, considering suitable $E_{1/2}$ reduction potentials in different electrolytic environments, the EA range varies between −3.91 and −4.00 eV. Notably, PTCDIPr shows slightly larger EA (ca. 0.1−0.2 eV) than BNPTCD.

The kinetics of the perylenediimide-based electrodes can be discussed by looking at the effect of the scan rate on the peak intensity and potential values. The CV diagrams of the BNPTCD LB film registered at scan rates in the 0.07−0.25 V s^{-1} range and using 0.1 mol L^{-1} aqueous $LiClO_4$ as supporting electrolyte are shown in Figure 6a. It can be seen that the higher the sweep rate values, the higher the peak currents for the film electrode. At the same time, increasing the scan rate promotes peak broadening and separation, indicating kinetic limitations in the multilayer films. This latter data points to a diffusion-controlled reaction. However, the peak intensity ratio in the reverse scan is maintained throughout this sweep rate range, suggesting a quasireversible electron transfer.

The peak currents plotted versus v and $v^{1/2}$, both the anodic and cathodic, are linear with v (Figure 6b,c) and $v^{1/2}$, respectively. This trend in the peak currents with the scan rate, and the appearance of diffusion tails (broadening and peak separation) in the CV responses, confirms that the electron transfer through these multilayer films is diffusion controlled. There is, however, a slightly different trend for the anodic and cathodic peak intensities with the scan rate: in the case of the v plots, both the slopes and linear regression coefficients are almost identical. On the other hand, the relation of the cathodic peak intensity—which involved the formation of anionic species—with $v^{1/2}$ is not the ideal fit ($r^2 = 0.949$), while the anodic has $r^2 = 0.983$, supporting the conclusion that the diffusion rate for cations through the thin film is a determining factor in the redox process. Similar diffusion-controlled processes were found for PTCDIPr LB.

3.2.3. Carbon Paste Electrodes (CPEs). Since most perylene derivatives are insoluble or only partially soluble in most organic solvents, the technique of carbon paste electroactive electrodes (CPEEs) was used.[23] The CPEs are the working electrodes in the voltammetric experiments, and the responses correspond to electrochemical transformations of the incorporated PTCD compound. The electrochemical behavior of BNPTCD and PTCDIPr as modifiers of the CPEs was recorded. The observed CV waves are considerably broader than those for LB films (Figure 7a), typical of the carbon paste technique, which is due to the complex heterogeneous nature of the CPEs. Generally, the presence of the hydrophobic binder at the electrode surface decreases the charge (mass) transfer rate, causing kinetics limitations. The CV diagrams recorded at 100 mV.s^{-1} of a BNPTCD-based CPE immersed in 0.1 mol L^{-1} KCl solution exhibits two reduction peaks, being localized

at ca. $E_{red1} = -0.55$ V and $E_{red2} = -0.95$ V, respectively (vs Ag/AgCl). It should be pointed out that the separation between reduction peaks, which has been interpreted as a measure of the twisting of the perylene core,[16] is 0.4 V, a value larger than the one measured from voltammograms in solution. The CV plots for PTCDIPr CPE immersed in 0.1 mol L^{-1} KCl solution, and recorded under identical experimental conditions as those used for BNPTCD, show the same overall behavior. The CV results for bulk CPE matrix could be attributed to a distinct packing of the two perylenediimides that may condition an inequivalent accessibility for the charge transfer. Similar CV patterns were obtained for CPE of PTCDIPr and BNPTCD in 0.1 mol L^{-1} $LiClO_4$ aqueous solutions, indicating that the effect of the electrolyte on reduction values is not as evident as occurs in CV of LB films.

The effect of the scan rate on the voltammetric response for the immobilized PTCDIPr into the carbonaceous matrix was studied and is illustrated in Figure 7a. With the scan rate spread from 0.02 V to 0.50 $V \cdot s^{-1}$, both the redox peak currents and peak-to-peak distance increase, suggesting a quasireversible solid-state redox reaction. The kinetics shows that diffusion of the electrolyte in the paste is not fast enough to keep the current level at those scan rates. Complementary information about the peak current versus scan rate (v) and the square root of the scan rate ($v^{1/2}$) was obtained in different electrolyte media. The curves of Figure 7b,c show that the peak current presents a good linear behavior with the $v^{1/2}$, with scan rate values between 0.02 and 0.20 V, confirming the assumption that the electron transfer is controlled by the diffusion of solution species. Clearly, the best linear fit is obtained at low scan rates (less than 100 $mV \cdot s^{-1}$), an observation that supports the interpretation of electron transfer kinetics as sluggish, where the redox processes depend mainly on the counterions' diffusion into the electrode. This fact suggests that perylenediimide molecules are randomly dispersed on the carbon paste suspension rather than adsorbed onto the conductive graphite particles.

In summary, a better resolution is achieved in the CV voltammograms of LB films compared with the CPE results; however, the CPE technique offers better reproducibility with consecutive scanning and is not affected by changes in the supporting electrolyte.

Conclusions

The cyclic voltammetry behavior of two perylenediimide derivatives in solid state and one of them in solution are reported here for the first time. The data collected permit a clear description of the main factors affecting electrochemical behavior: the degree of organization, electrode structure, and the supporting electrolyte. A comparison between the CV responses in CPE (random molecular distribution) and in highly organized LB films highlights the advantages and pitfalls of the techniques. LB films facilitate the electrochemical processes, enhanced sensitivity allowing better resolution of the CV peaks. The CPE technique offers reproducible results over consecutive scanning and a variety of supporting electrolytes. In summary, the two solid-state electrodes provide complementary information for solid-state electrochemical characterization. It is shown that the electron-transfer processes in both type of electrodes are diffusion-controlled. The reduction data are used to estimate the electron affinities of both derivatives, and the values are compared with those extracted from DFT calculations.

Acknowledgment. Financial support from CICYT (Grant no. AGL2001-2104-C02-01) is gratefully acknowledged. T.D.C. (F.P.U. fellowship) and R.F.A. (SAB2002-0017) acknowledge fellowships by the Spanish Ministry of Education-MEC-Spain.

CM0347786